



Derwent, R. G., Stevenson, D. S., Utembe, S. R. ., Jenkin, M. E., Khan, A. H., & Shallcross, D. E. (2020). Global modelling studies of hydrogen and its isotopomers using STOCHEM-CRI: Likely radiative forcing consequences of a future hydrogen economy. *International Journal of Hydrogen Energy*, 45(15), 9211-9221.  
<https://doi.org/10.1016/j.ijhydene.2020.01.125>

Peer reviewed version

License (if available):  
CC BY-NC-ND

Link to published version (if available):  
[10.1016/j.ijhydene.2020.01.125](https://doi.org/10.1016/j.ijhydene.2020.01.125)

[Link to publication record in Explore Bristol Research](#)  
PDF-document

This is the author accepted manuscript (AAM). The final published version (version of record) is available online via Elsevier at <https://www.sciencedirect.com/science/article/abs/pii/S0360319920302779#!>. Please refer to any applicable terms of use of the publisher.

## University of Bristol - Explore Bristol Research

### General rights

This document is made available in accordance with publisher policies. Please cite only the published version using the reference above. Full terms of use are available:  
<http://www.bristol.ac.uk/red/research-policy/pure/user-guides/ebr-terms/>

Global modelling studies of hydrogen and its isotopomers using STOCHEM-CRI: Likely radiative forcing consequences of a future hydrogen economy

Richard G. Derwent<sup>a,\*</sup>, David S. Stevenson<sup>b</sup>, Steven R. Utembe<sup>c</sup>, Michael E. Jenkin<sup>d</sup>, Anwar H. Khan<sup>e</sup>, Dudley E. Shallcross<sup>e</sup>

<sup>a</sup> rdscientific, Newbury, United Kingdom.

<sup>b</sup> School of Geosciences, University of Edinburgh, United Kingdom.

<sup>c</sup> Environmental Protection Authority, Melbourne, Victoria, Australia.

<sup>d</sup> Atmospheric Chemistry Services, Okehampton, United Kingdom.

<sup>e</sup> School of Chemistry, University of Bristol, Bristol, United Kingdom.

\* Corresponding author. rdscientific, Newbury, Berkshire RG14 6LH, United Kingdom.

E-mail addresses: r.derwent@btopenworld.com (R. Derwent), david.s.stevenson@ed.ac.uk (D. Stevenson), steven.utembe@epa.vic.gov.au (S. Utembe), atmos.chem@btinternet.com (M. Jenkin), anwar.khan@bristol.ac.uk (A. Khan), d.e.shallcross@bristol.ac.uk (D. Shallcross).

## Abstract

A global chemistry-transport model has been employed to describe the global sources and sinks of hydrogen (H<sub>2</sub>) and its isotopomer (HD). The model is able to satisfactorily describe the observed tropospheric distributions of H<sub>2</sub> and HD and deliver budgets and turnovers which agree with literature studies. We then go on to quantify the methane and ozone responses to emission pulses of hydrogen and their likely radiative forcing consequences. These radiative forcing consequences have been expressed on a 1 Tg basis and integrated over a hundred-year time horizon. When compared to the consequences of a 1 Tg emission pulse of carbon dioxide, 1 Tg of hydrogen causes  $5 \pm 1$  times as much time-integrated radiative forcing over a hundred-year time horizon. That is to say, hydrogen has a global warming potential (GWP) of  $5 \pm 1$  over a hundred-year time horizon. The global warming

consequences of a hydrogen-based low-carbon energy system therefore depend critically on the hydrogen leakage rate. If the leakage of hydrogen from all stages in the production, distribution, storage and utilisation of hydrogen is efficiently curtailed, then hydrogen-based energy systems appear to be an attractive proposition in providing a future replacement for fossil-fuel based energy systems.

## 1. Introduction

Hydrogen is widely recognised as an important future energy carrier because of its potential benefits through reduced pollutant and greenhouse gas emissions [1]. If, in the future, hydrogen were made from renewable energy sources, it would be possible to build an energy system with zero emissions of pollutants and greenhouse gases [2]. The elements of a future hydrogen economy have been reviewed in detail elsewhere [3] in terms of the production, storage, transmission, distribution and end-use of hydrogen. Currently, hydrogen storage is seen as a major difficulty in the transition from fossil-fuel based energy systems to a zero-carbon hydrogen economy [4].

Hydrogen ( $H_2$ ) is the simplest of all the molecular gases in the atmosphere. It is relatively unreactive and behaves as a well-mixed trace gas in the troposphere. The main atmospheric sources of hydrogen are the combustion of fossil fuels, biomass burning and the photochemical oxidation of methane and other organic compounds by way of the photolysis of formaldehyde, an important oxidation product. The main atmospheric sinks are uptake by soils and oxidation by tropospheric hydroxyl (OH) radicals which give hydrogen an atmospheric lifetime of the order of two years [5]. The element hydrogen has two stable isotopes: protium ( $^1H = H$ ) and deuterium ( $^2H = D$ ), both of which occur naturally in the atmosphere. Because of its relative rarity, deuterium is present essentially as the isotopomer HD and its abundance is characterised by the D/H ratio [5]. Atmospheric hydrogen has not been widely studied which is somewhat surprising in view of its possible importance as a future energy carrier.

Several studies in the 2000s raised the issue that a hydrogen economy would potentially lead to an increase in atmospheric hydrogen levels due to leakage from the hydrogen production, storage, transmission and distribution systems. This additional loading of atmospheric hydrogen could have impacts on the stratospheric ozone layer [6–11] and the

global climate system [12–14]. No further attention here is given to the depletion of the stratospheric ozone layer and attention is turned to the potential impacts of increased hydrogen levels on global climate change.

Hydrogen acts as an indirect greenhouse gas because of its reaction with tropospheric OH which depletes the oxidising capacity of the troposphere, and increases the atmospheric lifetimes of all the other trace gases which have OH oxidation as a main feature of their life cycles, such as methane [12]. Increased methane lifetimes will lead to increased greenhouse warming and, in turn, increased tropospheric ozone which is also a potent greenhouse gas. The IPCC 2001 [15] in their Third Assessment Report identified that in a possible fuel-cell economy, future hydrogen emissions may need to be considered as a potential climate perturbation. Over the last twenty year since the publication of the IPCC 2001 report, there have been few studies of the global climate consequences of increased hydrogen levels. The global environmental impacts from the application of hydrogen fuel cell technology to power the surface traffic fleet have been explored [13,14]. These studies postulated that an upper limit hydrogen leakage rate of 10% would lead to a small increase of about 4% in the contribution to greenhouse forcing from methane.

Derwent et al. 2006 [16] went on to show that a future hydrogen economy would indeed have greenhouse gas consequences and would not be free from climate perturbations. They estimated that if a global hydrogen economy were to replace the current fossil fuel-based system and exhibited a leakage rate of 1%, then it would produce a climate impact of 0.6% of the current fossil fuel-based system.

The accuracy of the above statements on the potential global warming impacts of a future hydrogen economy depend wholly on the adequacy and completeness of global models of hydrogen and these in turn depend on our understanding of the life cycle of atmospheric hydrogen and the processes that control it. Atmospheric process and budget studies provide the basis of the input data employed to build the atmospheric hydrogen models used to assess the global environmental consequences of a future hydrogen economy. The aim of this study is to describe the formulation and application of a global Lagrangian chemistry-transport model to address H<sub>2</sub> and HD and to use this model to estimate the indirect radiative forcing and global warming potential (GWP) of hydrogen.

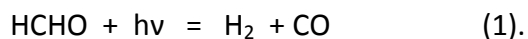
## 2. Methodology

### 2.1 STOCHEM-CRI model

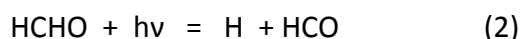
The STOchastic CHEMistry model is a global Lagrangian three-dimensional chemistry transport that was initially developed to describe the global distributions of ozone and methane [17]. A detailed description of the model together with its horizontal and vertical coordinates, advection scheme and meteorological parameterisations and datasets is given in Collins et al., 1997 [17]. This early version is called STOCHEM-OC. Subsequently the representation of the atmospheric chemistry of ozone, oxides of nitrogen, carbon monoxide, methane and a range of organic compounds has been expanded considerably by incorporating the Common Representative Intermediate (CRI) chemical mechanism [18] and this newer version is called STOCHEM-CRI. Use of this enhanced version is particularly important for the accurate global representation of H<sub>2</sub> and HD because the photochemical oxidation of methane and other organic compounds is the most important source of hydrogen. This is the STOCHEM version employed in this study and further details are given in Utembe et al., 2010 [19]. STOCHEM-CRI has been employed to describe the tropospheric distribution of ozone [19– 1] and of organic aerosol [22]. It has been used to explore different aspects of tropospheric chemistry involving formaldehyde [23], peroxyacetic acid [24], the ozonolysis of ethene [25], Criegee intermediates [26], methanol [27], organic peroxy radicals [28], organic hydroperoxides [29], acetone [30], nitrate radicals [31], alkyl nitrates [32], dimethyl sulphide [33], peroxyacetyl nitrate [34] and sesquiterpenes [35]. These studies each include a comprehensive comparison between observations and the predictions from STOCHEM-CRI.

### 2.2 Representation of the photochemical sources and sinks of H<sub>2</sub> and HD

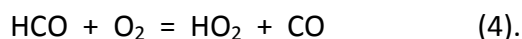
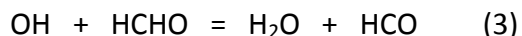
STOCHEM-CRI represents the chemistry of ozone, oxides of nitrogen, carbon monoxide (CO), methane and a wide range of organic compounds using 220 species and 609 chemical and photochemical reactions. The increased chemical complexity in the CRI mechanism allows STOCHEM-CRI to treat a wider range of emitted organic compounds and this is essential to the accurate representation of the main tropospheric hydrogen source which is the photolysis of formaldehyde (HCHO) in reaction (1):



There are two additional removal processes for HCHO in addition to reaction (1), neither of which generate hydrogen. The first is photolysis via reaction (2):



and the second is attack by OH in reaction (3):



As a result, the production of hydrogen depends critically on the competition between reactions (1) and (2)+(3)+(4) and so is highly spatially- and temporally-dependent, requiring a full three-dimensional model for its accurate representation.

The STOCHEM-CRI model version employed here was that assembled for the purposes of modelling sesquiterpenes and has been described in some detail elsewhere [35] with suitable extensions to enable the addressing of HD. Formaldehyde and hence H<sub>2</sub> and HD, is a by-product of the oxidation by OH and ozone of almost all atmospheric organic compounds. In the STOCHEM-CRI base case there are 22 emitted organic compounds: methane, formaldehyde, formic acid, methanol, ethane, ethene, acetylene, acetaldehyde, acetic acid, propane, propene, propionaldehyde, acetone, butane, methylethylketone, trans but-2-ene, isoprene, benzene, toluene, o-xylene, α-pinene and β-pinene. The oxidation of almost all of these model species contribute to or influence in some way, the photochemical production of formaldehyde.

The base case H<sub>2</sub> photochemical source strength was found to be about 49 Tg yr<sup>-1</sup> which is in the middle of the range of previous estimates (37 – 77 Tg yr<sup>-1</sup>) [36]. Using a D/H isotope ratio, δD, of 190 ‰ for photochemical production [37], where the isotope ratio is defined as:

$$\delta\text{D} = \frac{\text{D}/\text{H}}{\text{D}_{\text{smow}}/\text{H}_{\text{smow}}} - 1 \quad * \quad 1000 \quad (5).$$

and D<sub>smow</sub>/H<sub>smow</sub> is 0.015576 for Standard Mean Ocean water (SMOW) [38], gives a photochemical HD source strength of 0.91 Tg yr<sup>-1</sup>.

The main photochemical sinks for H<sub>2</sub> and HD in STOCHEM-CRI are the reactions with OH radicals. Again, the instantaneous fluxes through these reactions are highly spatially and temporally variable and so they can only be estimated accurately using a three-dimensional model. The base case H<sub>2</sub> photochemical sink was found to be about 16 Tg yr<sup>-1</sup> which is well within the range of previous estimates (15 – 22 Tg yr<sup>-1</sup>) [39] and that for HD was found to be about 0.3 Tg yr<sup>-1</sup>.

### 2.3 Representation of the soil uptake sink for H<sub>2</sub> and HD

Although the soil uptake sink for hydrogen is recognised as the dominant removal process, it is, however, relatively uncertain because of the large variety of soils and ecosystems that must be considered [5]. Because the majority of the soil sink lies in the northern hemisphere, hydrogen has an inverted concentration distribution [40]. That is to say, despite the preponderance of northern hemisphere sources, hydrogen concentrations are higher in the southern hemisphere because sinks are stronger in the northern hemisphere.

Soil uptake of H<sub>2</sub> and HD was treated in STOCHEM-CRI using a deposition velocity,  $v_g$ , approach such that the flux of hydrogen,  $F$ , from the atmosphere was described as:

$$F = v_g \cdot c \quad (6).$$

where  $c$  is the H<sub>2</sub> number density. An authoritative review of candidate  $v_g$  values for a range of soils and ecosystems is available [5]. Sanderson et al., 2003 [41] performed a detailed three-dimensional model analysis of hydrogen soil uptake, assigning  $v_g$  values to seven different types of ecosystem, estimating a global  $v_g$  of 0.53 mm s<sup>-1</sup> and a global sink strength of 58.3 Tg yr<sup>-1</sup>. An important feature of the Sanderson et al., 2003 study was the recognition of the importance of geographic and seasonal changes in soil moisture, snow cover and vegetation type.

The STOCHEM-CRI base case model assumed a constant  $v_g$  over land surfaces, a  $v_g$  of zero over ocean surfaces and set a temperature threshold so that surface uptake by frozen land surfaces was switched off. The value of  $v_g$  over land was chosen so that H<sub>2</sub> sources and sinks were in approximate balance and the model was able to reproduce accurately the annual average hydrogen mixing ratio observed at Mace Head, Ireland. The global H<sub>2</sub> surface uptake sink strength was found to be 79 Tg yr<sup>-1</sup> which is towards the high end of previous

estimates (54 – 88 Tg yr<sup>-1</sup>) [39] because of the higher photochemical hydrogen source strength employed here due to the increased coverage of VOCs and the requirement that sources and sinks should be in approximate balance. Using the isotopic fractionation factor of 0.943 [37], the global HD soil uptake sink strength was found to be 4.3 Tg HD yr<sup>-1</sup>.

#### 2.4 Emission sources of H<sub>2</sub>, HD and other trace gases

The global total emissions of H<sub>2</sub>, HD and a wide range of trace gases, together with their splits into the different source types, in the base case STOCHEM-CRI are given in Table 1. The assumed monthly 5° x 5° spatial distributions for the man-made sources are described elsewhere [17]. Emissions from biomass burning, vegetation, oceans, soils and ‘other’ sources were distributed using maps at 5° x 5° resolution [42]. The emissions of organic compounds were adapted from the Precursors of Ozone and their Effects in the Troposphere (POET) inventory [43] for the year 1998.

The base case H<sub>2</sub> emissions were set at 20 Tg yr<sup>-1</sup> from man-made sources and 20 Tg yr<sup>-1</sup> from biomass burning, see Table 1. Literature reviews [5] point to considerable uncertainty surrounding these figures not only in their absolute magnitudes but also in their spatial and seasonal distributions [39]. The base case emissions adopted here were at the top end of the ranges employed in previous modelling studies of hydrogen for man-made emissions (11 – 20 Tg yr<sup>-1</sup>) [39] and biomass burning (8 – 20 Tg yr<sup>-1</sup>) [39]. Taking the isotopic signatures, δD of -270 ‰ and -90 ‰, respectively, for man-made sources and biomass burning [37], base case HD emissions were found to be 0.28 Tg HD yr<sup>-1</sup> and 0.23 Tg HD yr<sup>-1</sup>, see Table 1.

### 3. Base case model results

#### 3.1 Global burdens and atmospheric lifetimes of the main tropospheric trace gases

Each STOCHEM-CRI model experiment was run for five years using meteorological data from a 1998 archive and the results were taken from the fifth and final complete year. The base case global burdens and atmospheric lifetimes are taken to be representative of the 2000s. The base case run gave a yearly-averaged methane burden of 4306 Tg and an atmospheric lifetime of 7.2 years. These estimates compare well with those from the STOCHEM-OC Monte Carlo uncertainty analysis of 4620 ± 460 Tg and 9.0 ± 4.6 years (where the quoted uncertainty ranges are 2 – σ or 95% confidence ranges) [21] but were lower than those from



the Atmospheric Chemistry Coupled Climate Model Intercomparison Project (ACCMIP) which gave  $4813 \pm 162$  Tg and  $9.7 \pm 3.0$  years [44]. Because the methane atmospheric lifetime was towards the lower end of the ACCMIP range, we must consider the possibility that this may have introduced bias into the estimated GWP for hydrogen and this is discussed later.

The yearly-averaged carbon monoxide burden in the base case was 408 Tg and the atmospheric lifetime was 45 days. These estimates compared well with those exhibited by the STOCHEM uncertainty analysis ( $374 \pm 209$  Tg;  $53 \pm 34$  days) [21] and is at the upper end of the ACCMIP ( $323 \pm 76$  Tg) [44] range.

The yearly-averaged tropospheric ozone burden (calculated where the ozone mixing ratio is less than 150 ppb [45]) was 321 Tg and the atmospheric lifetime was 28 days. Again, these estimates are within the ranges exhibited by STOCHEM-OC ( $262 \pm 127$  Tg;  $23.0 \pm 8$  days) [21] and within the range from ACCMIP ( $337 \pm 46$  Tg;  $22.3 \pm 4$  days) [44]. A tropospheric ozone burden of 328 Tg has been estimated from the Aura Ozone Monitoring Instrument (OMI) and the Microwave Limb Sounder (MLS) measurements [46]. The base case tropospheric ozone burden is therefore in good agreement with the satellite measurement.

The global burden and atmospheric lifetime of hydrogen in the base case were 150 Tg and 1.5 years, respectively. The burden estimate was well within the literature range [36], that is to say, 149 – 176 Tg and the atmospheric lifetime estimate was towards the lower end of the respective range, 1.4 – 2.7 years. It would appear that the base case model results present a regime in which hydrogen sinks are somewhat over-estimated, leading to a shorter atmospheric lifetime. The over-estimation of hydrogen sinks appeared to be associated with an over-estimation of the methane sinks.

### 3.2 Global surface distribution of hydrogen

An important test of global model performance is its ability to reproduce the observed spatial gradients and seasonal cycles of the well-mixed tropospheric gases. In this study, attention is focussed on the model's ability to reproduce the observed latitudinal distribution of hydrogen and the seasonal cycles in the mixing ratios at three baseline stations: Mace Head, Ireland ( $53.3^{\circ}\text{N}$ ,  $9.9^{\circ}\text{W}$ ); Mauna Loa, Hawaii ( $19.5^{\circ}\text{N}$ ,  $155.6^{\circ}\text{W}$ ); Cape

Grim, Tasmania (40.7°S, 144.7°E). Surface hydrogen mixing ratios for these comparisons were taken from Carbon Dioxide Information Analysis Center (CDIAC) [47].

The base case model was able to represent some features of the observed surface distribution of hydrogen in terms of general levels and latitudinal gradients. A detailed comparison with observations is presented in Figure S.1 of the Supplementary Information attached to this paper. The seasonal cycle in surface hydrogen at Mace Head Ireland was well predicted but those at Mauna Loa Hawaii and Cape Grim Tasmania were not. Whilst the northern hemisphere predictions were satisfactory, those for the southern hemisphere were unsatisfactory. As a result, the magnitude and seasonal cycle of the northern hemisphere – southern hemisphere interhemispheric gradient were not satisfactorily predicted by the model.

This less than satisfactory model performance for hydrogen should be seen in the light of our current understanding of hydrogen in the troposphere. Ehhalt and Rohrer 2009 in their review of tropospheric hydrogen cycle, remarked that some features of hydrogen in relation to carbon monoxide and methane were rather puzzling. They pointed out that the hydrogen concentration distribution is controlled largely by surface uptake whose uncertainties are still considerable, with the result that it is not possible to reconcile 3 – D analyses with inverse modelling. We have not been able to resolve these complex issues in this STOCHEM-CRI study, despite the passage of time since the Ehhalt and Rohrer 2009 review. Ehhalt and Rohrer 2009 nevertheless concluded that our knowledge of the tropospheric hydrogen cycle was solid enough to make reasonable predictions about the consequences of its perturbation and, on this basis, we have continued with the estimation of the GWP for hydrogen.

### 3.3 Global surface distribution of HD

In this section, the performance of STOCHEM-CRI is examined using the available observational data for the isotopomer HD. Early observations of the D – content of atmospheric hydrogen,  $\delta D - H_2$  [5] point to about  $70 \pm 30$  ‰ for 1967 – 1969 over Colorado, USA. More recent observations from surface stations, ship cruises and aircraft campaigns point to an average D – content of about 130 ‰ [48,49]. This is considered to be a real increase which has been driven by the growth in methane which produces  $H_2$  with a high D

– content [5]. A seasonal variation in the D – content of H<sub>2</sub> at Cheeka Peak Observatory, Washington State, USA has been reported [50] which peaks in the autumn and reaches a minimum in the spring. The northern hemisphere mean  $\delta D - H_2$  of the aircraft observations [37] was  $128.3 \pm 0.7 \text{ ‰}$  and the southern hemisphere value was  $135.9 \pm 1.1 \text{ ‰}$ . The global mean  $\delta D - H_2$  in the extended Pacific Ocean ship-borne dataset [51] was  $126 \pm \text{‰}$ .

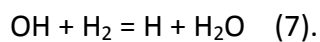
The base case model gave a good description of the ship-borne latitudinal profile of HD and was able to account for the location and magnitude of the drop in  $\delta D - H_2$  when moving from low latitudes of the southern hemisphere into the northern hemisphere as shown in Figure S.3 of the Supplementary Information. Generally, the base case model underestimated the aircraft observations with fractional biases of -0.2 to -0.3 and a detailed comparison is presented in the Supplementary Information. The base case model performed well in predicting the surface distribution of HD and because of the way in which the parameter  $\delta D - H_2$  exaggerates small differences in D/H ratios, the negative biases were of little statistical significance. It appears that STOCHEM model performance for HD was significantly better than that for hydrogen itself, supporting our view that our description of hydrogen in the troposphere was solid enough to warrant estimation of its GWP.

#### 4. Behaviour of hydrogen in responses to emission pulses

Central to the Global Warming Potential (GWP) concept is the behaviour of a trace gas in response to an emission pulse of that species. Accordingly, therefore, a pulse of H<sub>2</sub> was added to the model and its fate and behaviour were studied. STOCHEM-CRI was set up as described above and at a suitable point, two five-year model runs were initiated. One model run was a continuation of the base case, the base case scenario run. In the other five-year model run, the man-made emission of H<sub>2</sub> was increased across-the-board for a short period, with all other model inputs set up as in the base case. The emission perturbation amounted to an extra 1.67 Tg of H<sub>2</sub> was added during the first month and this was followed for the remainder of the five-year period. The size of the emission pulse was completely arbitrary but needed to be large enough to generate differences between the base case and perturbed scenario cases that were perceptible yet not too large as to move the modelling system out of its linear region. Because the air parcel positions and all other model input parameters remained unchanged, the emission pulse generated small but reproducible differences from the base case that could be accurately monitored and assessed.

The differences in trace gas mixing ratios, reaction fluxes and trace gas burdens between the base case and perturbed scenario cases were followed closely over the five-year time period. The differences in the global H<sub>2</sub> burdens started off at 1.67 Tg and declined steadily with an e-folding time of 1.52 years. This timescale is exactly the same as the atmospheric lifetime found for H<sub>2</sub> in the base case, see section 3.1 above. The perturbation applied to H<sub>2</sub> has therefore not significantly affected the main H<sub>2</sub> sink which is surface uptake. The H<sub>2</sub> pulse therefore decayed away with the same time constant as the tropospheric H<sub>2</sub> burden in the base case. For H<sub>2</sub> then, adjustment times and atmospheric lifetimes were found to be identical.

The perturbed scenario case had a small additional burden of H<sub>2</sub> which decayed away steadily during the five-year model run. During which time, its presence in the troposphere led to a small (0.8 %) increase in the flux through the OH + H<sub>2</sub> reaction (7):



This increased OH + H<sub>2</sub> reaction flux also decayed away with an e-folding time of 1.52 years, exactly the same time constant as that of the H<sub>2</sub> pulse, itself. Since OH radical sources and sinks are in some form of steady state, then this increased reaction flux led to a small decrease in the OH radical steady state. This, in turn, led to a small decrease in the OH + CH<sub>4</sub> reaction flux which, in turn, led to a build-up in the global burden of CH<sub>4</sub>, since the OH + CH<sub>4</sub> reaction is the main CH<sub>4</sub> removal process.

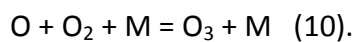
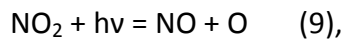
Figure 1 presents the time development of the divergence between the global mean CH<sub>4</sub> mixing ratios between the base case and perturbed scenario runs after the addition of a 1.67 Tg pulse of H<sub>2</sub>. The divergence increased steadily during the first and second model years but this rate of increase slowed during the third year and then began to level off, reaching a peak of about 0.080 ppb (80 ppt) during the spring of the fourth year. The divergence then began a slow decline during the remainder of the fourth and five years, with an e-folding time constant of between 10 and 20 years.

The sole fate of the hydrogen atoms produced in reaction (7) above is to react with oxygen to form the hydroperoxyl radical (HO<sub>2</sub>). Consequently, the addition of a pulse of H<sub>2</sub> leads to a slight increase in the rate of production of HO<sub>2</sub> radicals. Since HO<sub>2</sub> radicals are in some form of steady state, this increase in the rate of production must be met by an increase in

the rate of the HO<sub>2</sub> loss processes. There is therefore a slight increase in the rate of the reaction of HO<sub>2</sub> radicals with nitric oxide (NO) in reaction (8):



The HO<sub>2</sub> + NO reaction acts as a major source of tropospheric ozone through the photostationary state reactions (9)+(10):



The increased flux through the OH + H<sub>2</sub> reaction therefore leads to an increased rate of production of ozone (O<sub>3</sub>).

In Figure 2, the time development of tropospheric ozone is presented in response to an emission pulse of hydrogen. In this plot, the increased burden of ozone in the pulse scenario run, over and above that in the base case, is characterised using the difference in the global average ozone column densities between the model runs. At its peak, the difference in global average ozone column densities amounted to 0.0038 Dobson Units (DU), where 1 DU = 2.687 x 10<sup>16</sup> molecule cm<sup>-2</sup>, that is to say about 0.01 %. This difference exhibited a notable seasonal cycle and decayed away with an e-folding time scale of about 2 years in the first year, declining to about 3 years in subsequent years.

## 5. Radiative forcing consequences of hydrogen emission pulses and its GWP

Because H<sub>2</sub> is a homonuclear diatomic molecule, it lacks a dipole moment, does not absorb infrared radiation and so is not a direct radiatively active trace gas. However, it does react in the troposphere to perturb the global distributions of methane and tropospheric ozone, two important radiatively active trace gases and so it is classed as an indirect radiatively active trace gas. In this section, the global warming potential (GWP) of H<sub>2</sub> is estimated based on these indirect radiative consequences.

The GWP of a trace gas is defined as the ratio of the time-integrated radiative forcing resulting from the emission of 1 kg of the trace gas relative to that of 1 kg of carbon dioxide over a time horizon which is taken here to be 100 years [52]. That is to say:

T

$$\text{GWP} = \frac{\int_0^T a_i c_i dt}{\int_0^T a_{\text{CO}_2} c_{\text{CO}_2} dt} \quad (11),$$

where  $a_i$  is the instantaneous radiative forcing due to a unit increase in the concentration of trace gas,  $i$ , and  $c_i$  is the concentration of the trace gas,  $i$ , remaining after time  $t$  after its release and  $T$  is the number of years over which the calculation is performed. For  $\text{H}_2$ , the numerator has to be calculated from the impacts of the  $\text{H}_2$  pulses on methane and tropospheric ozone, since the direct impacts are zero.

To complete the calculation of the indirect GWP of hydrogen, we use the time development of methane and tropospheric ozone from section 4, the formula for the GWP in expression (11) and the radiative efficiency parameters  $a_{\text{CH}_4}$  and  $a_{\text{O}_3}$ . We took  $a_{\text{CH}_4}$  as  $3.63 \times 10^{-4} \text{ Wm}^{-2} \text{ ppb}^{-1}$  [53] which gave a peak radiative forcing in Figure 1 of  $0.029 \times 10^{-3} \text{ Wm}^{-2}$  for an  $\text{H}_2$  emission pulse of 1.67 Tg  $\text{H}_2$ . The time-integrated methane radiative forcing in the five-year model experiment was found to be  $0.067 \times 10^{-3} \text{ Wm}^{-2} \text{ year}$  per Tg  $\text{H}_2$ . To complete the GWP calculation, the time-integrated radiative forcing is required over the complete 100-year time horizon so the plot in Figure 1 needs to be extended over the remaining 95 years. This time extension was not possible with STOCHEM-CRI because of the long run time involved. However, the methane response could be extended to the end of the time horizon using the concept of trace gas adjustment timescales.

Emission pulses of the majority of trace gases decay away with e-folding timescales that are the same as their atmospheric lifetimes. However, methane increments tend to deplete the hydroxyl radical steady state concentrations and so slow up the decay of the methane pulses. The e-folding timescale of the decay of the methane pulses is called the methane adjustment timescale and it is about one quarter as long again as the methane atmospheric lifetime. A separate experiment was performed with STOCHEM-CRI to determine the methane adjustment time from its response to a 18 Tg methane emission pulse. The methane adjustment time in the base case model was found to be  $9.0 \pm 0.7$  years, that is to say, it is a factor of 1.25 times longer than the base case atmospheric lifetime. This factor is known as the feedback factor or methane adjustment factor and literature values lie within

the range from 1.23 – 1.35 [54]. The methane adjustment factor found here is well inside this literature range.

The time development of the methane radiative forcing in Figure 1 was therefore extended forward over the 100-year time horizon by assuming the peak radiative forcing decayed away with the methane adjustment time. This time extension added a further time integrated radiative forcing of  $0.145 \times 10^{-3} \text{ Wm}^{-2}\text{year}$  to the  $0.067 \times 10^{-3} \text{ Wm}^{-2}\text{year}$  per 1 Tg  $\text{H}_2$  from the first five years, making a total of  $0.21 \times 10^{-3} \text{ Wm}^{-2}\text{year}$  per 1 Tg  $\text{H}_2$ , which is considerably lower than the literature value of  $0.35 \times 10^{-3} \text{ Wm}^{-2}\text{year}$  [12].

Stevenson et al., 2013 [54] describe how to calculate the radiative forcing consequences from changes in the distribution of tropospheric ozone. They start by characterising the ozone column amounts on a  $5^\circ$  latitude x  $5^\circ$  longitude grid in Dobson Units (DU) and used a complex radiation code to relate these column amounts to radiative forcings. We used the Stevenson et al., 2013 gridded estimates of radiative forcing per DU to estimate the radiative forcing consequences of the changes in tropospheric ozone column amounts resulting from the emission pulses of  $\text{H}_2$  presented in Figure 2. In response to a 1.67 Tg  $\text{H}_2$  emission pulse, the ozone response increased to a maximum of 0.0037 DU before decaying away. This response drove a change in radiative forcing which exactly mirrored the DU changes, reaching a peak radiative forcing of  $0.13 \times 10^{-3} \text{ Wm}^{-2}$ , also shown in Figure 2. The time-integrated forcing during the first five years amounted to  $0.151 \times 10^{-3} \text{ Wm}^{-2}\text{year}$  per 1 Tg  $\text{H}_2$ . Extension to the 100-year time horizon amounted to a further  $0.040 \times 10^{-3} \text{ Wm}^{-2}\text{year}$ , based on the 3-year e-folding time found for the tropospheric ozone adjustment time in Figure 4. The total radiative forcing from the tropospheric ozone response amounted to  $0.19 \times 10^{-3} \text{ Wm}^{-2}\text{year}$  per 1 Tg  $\text{H}_2$ . This estimate here is somewhat smaller than the literature value of  $0.25 \times 10^{-3} \text{ Wm}^{-2}\text{year}$  [12].

To calculate the GWP for hydrogen, the numerator of expression (11) was formed by adding together the methane and tropospheric ozone forcing terms to make  $0.40 \times 10^{-3} \text{ Wm}^{-2}\text{year}$  and dividing by the denominator, which was taken to be  $9.17 \times 10^{-5} \text{ Wm}^{-2}\text{year}$  [53], giving 4.4 over a 100-year time horizon. This value is considerably less than our literature value of 5.8 from nearly twenty years ago [12] but in good agreement with our reassessment of this earlier GWP study which found a  $2 - \sigma$  confidence range of 0 – 10 about a central value of 4.3 [55].

## 6. Sensitivity of the GWP to the base case assumptions

An important issue remaining is whether our particular choice of base case has introduced any hidden bias in the estimated GWP for hydrogen despite it employing “best estimate” model input data. Because the methane atmospheric lifetime was towards the bottom end of the ACCMIP range [44], we must consider the possibility that this has indeed introduced bias into our estimated GWP. This issue is part of our wider concern about the uncertainties in global model output when used for policy purposes [55]. In previous work, we have employed Monte Carlo uncertainty analysis techniques to the estimation of confidence limits of our predictions of the global burdens and atmospheric lifetimes of methane, carbon monoxide and ozone. We have drawn from this study, an “alternative”, plausible base case and followed the identical methodology to redetermine the GWP for hydrogen. In this way, we have been able to answer the question as to whether the base case assumptions have significantly influenced our estimate for the GWP for hydrogen.

Accordingly, an “alternative” base case was set up by changing the emissions, stratospheric ozone input, temperature and water vapour biases. This “alternative” base case gave a methane atmospheric lifetime of 10.4 years which is significantly longer than the “best estimate” base case. This gives a significantly improved comparison with the ACCMIP models which reported  $9.7 \pm 3.0$  years [44]. The tropospheric ozone burden in the “alternative” base case was found to be 388 Tg which is significantly higher than the “best estimate” base case of 321 Tg and the satellite observations [46] which reported 328 Tg. In summary, the “alternative” base case offered improved model performance for the methane lifetime at the detriment of model performance for the tropospheric ozone burden. It certainly, however, should shed light on the issues raised in section 3.1 above concerning any bias introduced into the GWP estimation from the base case model assumptions.

With the “alternative” base case assumptions, initial methane responses to the hydrogen emission pulse were somewhat smaller and took longer to reach a peak, with the result that the integrated methane response over the 5-year model experiment was about 16% lower. However, the methane response over the last year of the model experiment was only 8% lower because of the longer time to reach the peak. The methane adjustment time was significantly longer compared with that in the base case so that the time-integrated



methane response between 5 and 100 years was significantly higher, by about 34%. Overall the total methane response was  $0.25 \text{ mWm}^{-2} \text{ years}$  per 1 Tg in the “alternative” base case compared with  $0.21 \text{ mWm}^{-2} \text{ years}$  per 1 Tg in the “best estimate” base case, that is to say, 19% higher.

Initial ozone responses to the hydrogen emission pulse were slightly larger in the “alternative” base case but there was little significant difference in the peak responses. Ozone responses decayed slightly more slowly so that the integrated ozone response over the 5-year model experiment was about 1% higher. The ozone adjustment time was about 1% longer so that the total ozone response was  $0.195 \text{ mWm}^{-2} \text{ years}$  per 1 Tg in the “alternative” base case compared with  $0.192 \text{ mWm}^{-2} \text{ years}$  per 1 Tg in the “best estimate” base case, about 1.5% higher.

Combining the methane and ozone responses, we estimate the GWP for hydrogen over the 100-year time horizon is 4.9 compared with 4.4 over the 100-year time horizon, that is to say 10% higher. On this basis, our best estimate of the GWP for hydrogen over a 100-year time horizon is 4.6, based on the average from the two base cases. This value is 20 % lower than our previous estimate of 5.8 from nearly twenty years ago [12]. Assuming a logarithmic relationship between GWP and methane lifetime and the  $2 - \sigma$  confidence range for the methane lifetime from our Monte Carlo uncertainty analysis, we estimate a  $2 - \sigma$  confidence range for the GWP for hydrogen to be  $4.6^{+0.6}_{-0.8}$  over a 100-year time horizon. Although this estimate takes into account any biases due to under- and over-prediction of the methane lifetime, it does not take into account any potential biases in our two base cases resulting from the problems we have highlighted in section 3.2 due to our inadequate description of the hydrogen cycle in the troposphere. An assessment of any potential biases due to our model description of hydrogen must await an improvement in this basic understanding. It is likely then that this  $2 - \sigma$  confidence range understates the real uncertainty range in the GWP.

Because of the inherent uncertainties in global CTMs, it is not straightforward to say whether the differences in GWPs between this study and our earlier work [12] has any real policy significance. In view of these uncertainties, our  $2 - \sigma$  confidence intervals need to be somewhat larger and our best estimate for the GWP of  $\text{H}_2$  becomes,  $5 \pm 1$  for a 100-year time horizon. That is to say, the emission of 1 Tg/yr of  $\text{H}_2$  causes the global warming

equivalent to  $5 \pm 1$  Tg/yr of CO<sub>2</sub>, when evaluated over a 100-year time horizon. Our judgment is that there is little real difference between this estimate and our previous estimate when the uncertainties in global CTM models for H<sub>2</sub> are taken into account.

## 7. Radiative forcing consequences of a future hydrogen economy

In this study, a global chemistry-transport model (CTM) has been used to calculate the likely magnitude of the radiative forcing impacts of emission pulses of H<sub>2</sub> through changes in the tropospheric distributions of methane and ozone. These radiative impacts have been expressed using the global warming potential concept. That is to say, the radiative forcing consequences of a 1 Tg emission pulse of H<sub>2</sub> has been expressed relative to a 1 Tg pulse of carbon dioxide (CO<sub>2</sub>) when integrated over a 100-year time horizon. The GWP of H<sub>2</sub> was found to be  $5 \pm 1$  for a 100-year time horizon. That is to say, the emission of 1 Tg/yr of H<sub>2</sub> causes the global warming equivalent to  $5 \pm 1$  Tg/yr of CO<sub>2</sub>, when evaluated over a 100-year time horizon.

To illustrate the potential consequences of a future hydrogen economy, we begin on the small scale by examining the consequences of replacing natural gas with hydrogen in the domestic sector of the United Kingdom. We consider only the H<sub>2</sub> emissions from leakage and leave out a number of potential other emission sources associated with upstream processing of fuels, electricity grid emissions and infrastructure. The UK domestic sector in 2011 accounted for 293,400 GWh of energy consumption [56] as natural gas and emitted 54.0 million tonnes CO<sub>2</sub> from the combustion products alone, ignoring the radiative forcing impacts from the methane released from natural gas leakage. If this 2011 domestic sector energy consumption were to be supplied on some future date by a low-carbon hydrogen system supplying hydrogen with an energy content of 142.18 MJ per kg [57] instead of natural gas, then 7.43 million tonnes of hydrogen would be required annually.

If this future hydrogen system was a perfectly sealed system with no leakage then it would save the entire 54.0 million tonnes of CO<sub>2</sub> per year, that is to say, the low-carbon H<sub>2</sub> system offers the potential for generating savings in greenhouse gas emissions of 54.0 million tonnes of CO<sub>2</sub> per year. If there were to be significant atmospheric leakage of H<sub>2</sub> from the production, distribution and end-use in the low-carbon system then the indirect global warming from hydrogen would reduce or offset some of the above savings in greenhouse

gas emissions. This reduction or offsetting can be estimated using the GWP for H<sub>2</sub> which is 5 ± 1 Tg of CO<sub>2</sub> per Tg of H<sub>2</sub>. On this basis, if there were to be a 1% leakage rate by mass, then this H<sub>2</sub> would have an equivalent global warming of 0.37 million tonnes CO<sub>2</sub> annually, reducing the savings in greenhouse gas emissions from 54.0 to 53.6 million tonnes CO<sub>2</sub> per year, that is by 0.7%. If there were to be a 10% leakage by mass, then this would offset the savings in greenhouse gas emissions by 7%. There is, therefore, an important potential savings in greenhouse gas emissions to be made by replacing natural gas by H<sub>2</sub> in the UK domestic sector at some point in the future, if H<sub>2</sub> leakage can be efficiently curtailed.

On the global scale, we estimate that the global H<sub>2</sub> production capacity required to replace the entire current fossil-fuel based energy system is about 2 500 Tg H<sub>2</sub> yr<sup>-1</sup> [16]. If there was a global leakage rate of 1%, then the global H<sub>2</sub> economy would have a radiative forcing impact of 125 Tg CO<sub>2</sub> yr<sup>-1</sup> over a 100-year time horizon. The fossil fuel system it replaces has a CO<sub>2</sub> emission of 23 000 Tg yr<sup>-1</sup>. Therefore, the global hydrogen economy with a 1% leakage rate has a radiative forcing impact of 0.5% of the fossil fuel system it replaces. If the leakage rate was 10%, then the radiative forcing impact would be 5% of the fossil fuel system.

## 8. Conclusions

This study has shown that H<sub>2</sub> itself, in contrast with most expectations, is a greenhouse gas and we have quantified its global warming potential relative to CO<sub>2</sub>. Indeed, this present assessment differs by a small margin (about 10 - 20%) from our previous work, despite the many advances in understanding of the fate and behaviour of H<sub>2</sub> over the past twenty years or so. We went on to quantify the global warming consequences of replacing the current fossil-fuel based energy system with one based on H<sub>2</sub> by considering small-scale and large-scale examples. The conclusion reached is that if the leakage of H<sub>2</sub> from all stages in the H<sub>2</sub> production, distribution, storage and utilisation is efficiently curtailed, then H<sub>2</sub>-based energy systems appear to be an attractive proposition in providing a future replacement for fossil fuel-based energy systems.

## Acknowledgements

RGD wishes to thank the Department of Business, Energy and Industrial Strategy for their support for the preparation of a review on the environmental impacts of hydrogen use in the UK domestic sector.

## References

- [1] Ogden JM. Prospects for building a hydrogen energy infrastructure. *Ann Rev Energy Environ* 1999; 24:227-279. <https://doi.org/10.1146/annurev.energy.24.1.227>.
- [2] Popa ME, Segers AJ, Denier van der Gon HAC, Krol MC, Visschedijk AJH, Schaap M, Rockmann T. Impact of a future H<sub>2</sub> transportation on atmospheric pollution in Europe. *Atmos Environ* 2015; 113, 208-222.
- [3] UNEP. The hydrogen economy. A non-technical review. DTI-0762-PA. Division of Technology, Industry and Economics, United Nations Environment Program, Paris. 2006.
- [4] Abe JO, Popoola API, Ajenifuja E, Popoola OM. Hydrogen energy, economy and storage: Review and recommendation. *Int J Hyd Energy* 2019; 44, 15072-15086.
- [5] Ehhalt DH, Rohrer F. The tropospheric cycle of H<sub>2</sub>: a critical review. *Tellus* 2009; 61B, 500-535.
- [6] Jacobson MZ. Effects of wind-powered hydrogen fuel cell vehicles on stratospheric ozone and global climate. *Geophys Res Lett* 2008;35, L19803, doi:10.1029/2008GL035102.
- [7] Tromp TK, Shia R-L, Allen M, Eiler JM, Yung YL. Potential environmental impact of a hydrogen economy on the stratosphere. *Science* 2003;300, 1740-1742.
- [8] van Ruijven B, et al. Emission scenarios for a global hydrogen economy and the consequences for global air pollution. *Global Environ Change* 2011; 21, 983-994.
- [9] Vogel B, Feck T, Groß J-U. Impact of stratospheric water vapor enhancements caused by CH<sub>4</sub> and H<sub>2</sub>O increase on polar ozone loss. *J Geophys Res* 2011;116, D05301, doi:10.1029/2010JD014234.
- [10] Wang D, Jia W, Olsen SC, Wuebbles DJ, Dubey MK, Rockett A.A. Impact of a future H<sub>2</sub>-based road transportation sector on the composition and chemistry of the atmosphere – Part 2: Stratospheric ozone. *Atmos Chem Phys* 2013;13, 6139-6150.
- [11] Warwick NJ, Bekki S, Nisbet EG, Pyle JA. Impact of a hydrogen economy on the stratosphere and troposphere studied in a 2-D model. *Geophys Res Lett* 2004; 31, L05107, doi:10.1029/2003GL019224.

- [12] Derwent RG, Collins WJ, Johnson CE, Stevenson DS, 2001. Transient behaviour of tropospheric ozone precursors in a global 3-D CTM and their indirect greenhouse effects. *Clim Change* 2001;49, 463-487.
- [13] Prather MJ. An environmental experiment with H<sub>2</sub>? *Science* 2003; 302, 58-59.
- [14] Schultz MG, Diehl T, Brasseur GP, Zitte, W. Air pollution and climate-forcing impacts of a global hydrogen economy. *Science* 2003;302, 624-627.
- [15] IPCC. *Climate Change 2001: The scientific basis*. pp. 256. Cambridge University Press, Cambridge, UK. 2001.
- [16] Derwent R, Simmonds P, O'Doherty S, Manning A, Collins W, Stevenson D. Global environmental impacts of the hydrogen economy. *Int J Nucl Hyd Prod Appl* 2006; 1, 57-67.
- [17] Collins WJ, Stevenson DS, Johnson CE, Derwent RG. Tropospheric ozone in a global-Scale three-dimensional Lagrangian model and its response to NO<sub>x</sub> emission controls. *J Atmos Chem* 1997;26, 223-274.
- [18] Jenkin ME, Watson LA, Utembe SR, Shallcross DE. A Common Representative Intermediates (CRI) mechanism for VOC degradation. Part 1: Gas phase mechanism development. *Atmos Environ* 2008;42, 7185-7195.
- [19] Utembe SR, Cooke MC, Archibald AT, Jenkin ME, Derwent RG, Shallcross DE. Using a reduced Common Representative Intermediates (CRI v2-R5) mechanism to simulate tropospheric ozone in a 3-D Lagrangian chemistry transport model. *Atmos Environ* 2010;13, 1609-1622.
- [20] Derwent RG, Utembe SR, Jenkin ME, Shallcross DE. Tropospheric ozone production regions and the intercontinental origins of surface ozone over Europe. *Atmos Environ* 2015;112, 216-224.
- [21] Derwent RG, Parrish DD, Galbally IE, Stevenson DS, Doherty RM, Naik V, Young PJ. Uncertainties in model of tropospheric ozone based on Monte Carlo analysis: Tropospheric ozone burdens, atmospheric lifetimes and surface distribution. *Atmos Environ* 2018;180, 93-102.

- [22] Utembe SR, Cooke MC, Archibald AT, Shallcross DE, Derwent RG, Jenkin ME. Simulating secondary organic aerosol in a 3-D Lagrangian chemistry transport model using the reduced Common Representative Intermediate mechanism (CRI v2-R5). *Atmos Environ* 2011;45, 1604-1614.
- [23] Cooke MC, Utembe SR, Carbajo PC, Archibald AT, Orr-Ewing AJ, Jenkin ME, Derwent RG, Lary DJ, Shallcross DE, 2010. Impacts of formaldehyde photolysis rates on tropospheric chemistry. *Atmos Sci Lett* 2010; 11, 33-38.
- [24] Bacak A, Cooke MC, Bardwell MW, McGillen MR, Archibald AT, Huey LG, Tanner D, Utembe SR, Jenkin ME, Derwent RG, Shallcross DE, Percival CJ. Kinetics of the  $\text{HO}_2 + \text{NO}_2$  reaction: On the impact of new gas-phase kinetic data for the formation of  $\text{HO}_2\text{NO}_2$  on  $\text{HO}_x$ ,  $\text{NO}_x$  and  $\text{HO}_2\text{NO}_2$  levels in the troposphere. *Atmos Environ* 2011;45, 6414-6422.
- [25] Leather KE, McGillen MR, Cooke MC, UtembeSR, Archibald AT, Jenkin ME, Derwent RG, Shallcross DE. Acid-yield measurements of the gas-phase ozonolysis of ethene as a function of humidity using chemical ionisation mass spectrometry. *Atmos Chem Phys* 2012;12, 469-479.
- [26] Percival CJ, Welz O, Eskola AJ, Savee JD, Osborn DL, Topping DO, Lowe D, Utembe SR, Bacak A, McFiggans G, Cooke MC, Xiao P, Archibald AT, Jenkin ME, Derwent RG, Riipinen I, Mok DWK, Lee EPF, Dyke JM, Taatjes CA, Shallcross DE. Regional and global impacts of Criegee intermediates on atmospheric sulphuric acid concentrations and first steps of aerosol formation. *Faraday Discuss* 2013;105, 45-73, DOI: 10.1039/c3fd00048f.
- [27] Khan MAH, Cooke MC Utembe SR, Xiao P, Derwent RG, Jenkin ME, Archibald AT, Maxwell P, Morris WC, South N, Percival CJ, Shallcross DE. Reassessing the photochemical production of methanol from peroxy radical self and cross reactions using the STOCHEM-CRI global chemistry and transport model. *Atmos Environ* 2014;99, 77-84.
- [28] Khan MAH, Cooke MC, Utembe SR, Archibald AT, Derwent RG, Jenkin ME, Morris WC, South N, Hansen JC, Francisco JS, Percival CJ, Shallcross DE. Global analysis of peroxy radicals and peroxy radical-water complexation using the STOCHEM-CRI global chemistry and transport model. *Atmos Environ* 2015;106, 278-287.

- [29] Khan MAH, Cooke MC, Utembe SR, Xiao P, Morris WC, Derwent RG, Archibald AT, Jenkin ME, Percival CJ, Shallcross DE. The global budgets of organic hydroperoxides for present and pre-industrial scenarios. *Atmos Environ* 2015;110, 65-74.
- [30] Khan MAH, Cooke MC, Utembe SR, Archibald AT, Maxwell P, Morris WC, Xiao P, Derwent RG, Jenkin ME, Percival CJ, Walsh RC, Young TDS, Simmonds PG, Nickless G, O'Doherty S, Shallcross DE. The global atmospheric budget and distribution of acetone using the 3-D global model, STOCHEM-CRI. *Atmos Environ* 2015;112, 269-277.
- [31] Khan MAH, Cooke MC, Utembe SR, Archibald AT, Derwent RG, Xiao P, Percival CJ, Jenkin ME, Morris WC, Shallcross DE. Global modelling of the nitrate radical ( $\text{NO}_3$ ) for present and pre-industrial scenarios. *Atmos Res* 2015;164-165, 347-357.
- [32] Khan MAH, Cooke MC, Utembe SR, Morris WC, Archibald AT, Derwent RG, Jenkin ME, Orr-Ewing AJ, Higgins CM, Percival CJ, Leather KE, Shallcross DE. Global modelling of the  $\text{C}_1 - \text{C}_3$  alkyl nitrates using STOCHEM-CRI. *Atmos Environ* 2015;123, 256-267.
- [33] Khan MAK, Gillespie SMP, Razis B, Xiao P, Davies-Coleman MT, Percival CJ, Derwent RG, Dyke JM, Ghosh MV, Lee EPF, Shallcross DE. A modelling study of the atmospheric chemistry of DMS using the global model STOCHEM-CRI. *Atmos Environ* 2016;127, 69-79.
- [34] Khan MAH, Cooke MC, Utembe SR, Archibald AT, Derwent RG, Jenkin ME, Leather KE, Percival CJ, Shallcross DE, 2017. Global budget and distribution of peroxyacetyl nitrate (PAN) for present and pre-industrial scenarios. *Int J Earth Environ Sci* 2017;2, 130-140.
- [35] Khan MAH, Jenkin ME, Foulds A, Derwent RG, Percival CJ, Shallcross DE. A modelling study of secondary organic aerosol formation from sesquiterpenes using the STOCHEM global chemistry and transport model. *J Geophys Res* 2017;122, doi:10.1002/2016JD026415.
- [36] Pieterse G, Krol MC, Batenburg AM, Brenninkmeijer CAM, Popa ME, O'Doherty S, Grant A, Steele LP, Krummel PB, Langenfelds RL, Wang HJ, Vermeulen AT, Schmidt M, Yver C, Jordan A, Engel A, Fisher RE, Lowry D, Nisbet EG, Reimann S, Vollmer MK, Steinbacher M, Hammer S, Forster G, Sturges WT, Rockmann T. Reassessing the variability in atmospheric  $\text{H}_2$  using the two-way nested TM5 model. *J Geophys Res* 2013;118, 3764-3780.
- [37] Rhee TS, Brenninkmeijer CAM, Rockmann T. The overwhelming role of soils in the global atmospheric hydrogen cycle. *Atmos Chem Phys* 2006;6, 1611-1625.

- [38] Hagemann R, Nief G, Roth E. Absolute isotopic scale for deuterium analysis of natural waters. Absolute D/H ratio for SMOW. *Tellus* 1970;22, 712-715.
- [39] Pieterse G, Krol MC, Batenburg AM, Steele LP, Krummel PB, Langenfelds RL, Rockmann T. Global modelling of H<sub>2</sub> mixing ratios and isotopic compositions with the TM5 model. *Atmos Chem Phys* 2011;11, 7001-7026.
- [40] Novelli PC, Lang PM, Masarie KA, Hurst DF, Myers R, Elkins JW. Molecular hydrogen in the troposphere: Global distribution and budget. *J Geophys Res* 1999;104, 30,427-30,444.
- [41] Sanderson MG, Collins WJ, Derwent RG, Johnson CE. Simulation of global hydrogen levels using a Lagrangian three-dimensional model. *J Atmos Chem* 2003;46, 15-28.
- [42] Olivier JG, Bouwman AF, Berdowski JJ, Veldt C, Bloos JP, Visschedijk AJ, Zandveld PY, Haverlag JL. Description of EDGAR Version 2.0: A set of global emission inventories of greenhouse gases and ozone-depleting substances for all anthropogenic and most natural sources on a per country basis and on 1 degree × 1 degree grid. Technical report, Netherlands Environmental Assessment Agency. 1996.
- [43] Granier C, Lamarque JF, Mieville A, Muller JF, Olivier J, Orlando J, Peters J, Petron G, Tyndall S, Wallens S. POET, a database of surface emissions of ozone precursors, <http://www.aero.jussieu.fr/project/ACCENT/POET.php>. 2005.
- [44] Naik V, Voulgarakis A, Fiore AM, Horowitz LW, Lamarque J-F, Lin M, Prather MJ, Young PJ, Bergmann D, Cameron-Smith J, Cionni I, Collins WJ, Dalsoren SB, Doherty R, Eyring V, Faluvegi G, Folberth GA, Josse B, Lee YH, MacKenzie IA, Nagashima T, van Noije TPC, Plummer DA, Righi M, Rumbold ST, Skeie R, Shindell DT, Stevenson DS, Strode S, Sudo K, Szopa S, Zeng G. Pre-industrial to present-day changes in tropospheric hydroxyl and methane lifetime from the Atmospheric Chemistry and Climate Model Intercomparison Project (ACCMIP). *Atmos Chem Phys* 2013;13, 5277-5298.
- [45] Stevenson DS, Doherty RM, Sanderson MG, Collins WJ, Johnson CE, Derwent RG. Radiative forcing from aircraft NO<sub>x</sub> emissions: Mechanisms and seasonal dependence. *J Geophys Res* 2004;109, D17307, doi:10.1029/2004JD004759.



- [46] Ziemke JR, Chandra S, Labow GJ, Bhartia PK, Froidevaux L, Witte JC. A global climatology of tropospheric and stratospheric ozone derived from Aura OMI and MLS measurements. *Atmos Chem Phys* 2011;11, 9237-9251.
- [47] CDIAC. Carbon Dioxide Information and Analysis Center. <https://cdiac.ess-dive.lbl.gov/hydrogen.html>. 2018.
- [48] Gerst S, Quay P. The deuterium content of atmospheric molecular hydrogen: method and initial measurements. *J Geophys Res* 105; 26433-26445.
- [49].Gerst S, Quay P. Deuterium component of the global molecular hydrogen cycle. *J Geophys Res* 106; 5021-5031.
- [50] Price H, Jaegle L., Rice A, Quay P, Novelli PC, Gammon R. Global budget of molecular hydrogen and its deuterium content: constraints from ground station, cruise and aircraft observations. *J Geophys Res* 2007; 112, D22108, doi:10.1029/2006JD008152.
- [51] Rice A, Quay P, Stutsman J, Gammon R, Price H, Jaegle L. Meridional distribution of molecular hydrogen and its deuterium content in the atmosphere. *J Geophys Res* 201;115, D12306, doi:10.1029/2009JD012529.
- [52] IPCC. *Climate Change: The IPCC Scientific Assessment*. Chapter 2. Cambridge University Press, Cambridge, UK. 1990.
- [53] IPCC. *Climate Change 2013: The Physical Science Basis*. Appendix 8.A, Cambridge University Press, Cambridge, UK. 2018.
- [54] Stevenson DS, + 34 co-authors. Tropospheric ozone changes, radiative forcing and attribution to emissions in the Atmospheric Chemistry and Climate Model Intercomparison Project (ACCMIP). *Atmos Chem Phys* 2013;13, 3063-3085.
- [55] Derwent RG. *Hydrogen for heating: Atmospheric impacts*. BEIS Research Paper: No. 18, Department for Business, Energy & Industrial Strategy, London. 2018.
- [56] DUKES. *Digest of UK Energy Statistics 2014*. Department of Energy & Climate Change, London. 2014.
- [57] Argonne National Laboratory. *Lower and higher heating values of hydrogen and fuels*. Hydrogen Analysis Resource Center, Argonne National Laboratory, Illinois, USA. 2008.